Macromolecular Research, Vol. 16, No. 1, pp 51-56 (2008)

On the Selection of FCC and BCC Lattices in Poly(styrene-*b*-isoprene) Copolymer Micelles

Joona Bang*

Department of Chemical and Biological Engineering, Korea University, Seoul 136-701, Korea

Timothy P. Lodge*

Department of Chemical Engineering & Materials Science, and Department of Chemistry, University of Minnesota, Minneapolis, MN 55455-0431

Received August 8, 2007; Revised August 31, 2007

Abstract: Spherical micelles of poly(styrene-*b*-isoprene) (SI) diblock copolymers in selective solvents have been reported to pack onto either face-centered cubic (fcc) or body-centered cubic (bcc) lattices. The selection rule for fcc and bcc lattices has been understood in terms of the intermicellar potentials, and they have been quantified using the ratio of the corona layer thickness to the core radius, L/R_c, as suggested by McConnell and Gast. In order to test the validity of the McConnell-Gast criterion, this study compared the L/R_c values from various solutions i.e. nine SI copolymers in several different selective solvents. The McConnell-Gast criterion was not found to be a determining factor, even though it could explain the fcc/bcc selection qualitatively. From the phase diagrams, the transition between fcc and bcc phases was also considered as a function of concentration and temperature, and their physical mechanisms are discussed based on the recent mean-field calculation reported by Grason.

Keywords: block copolymer micelle, order-order transition, face-centered cubic, body-centered cubic.

Introduction

Block copolymers in solution have been explored extensively due to their potential applications, including detergents, nanocarriers for drug delivery, modifying the flow properties of solutions, synthesis of nanocrystals, etc.[1-5] When dissolved in a selective solvent, block copolymers are well-known to self-assemble into micelles with various microstructures, such as vesicles, cylinders, and spheres.[1,2] Upon increasing concentration, they then pack into ordered structures, i.e., lamellae, hexagonally packed cylinders, and cubic-packed spheres.[1,2] In the case of spherical micelles, the most prevalent phases observed are close-packed (either face-centered cubic (fcc) or hexagonally close-packed (hcp)) and body-centered cubic (bcc) lattices. Of the particular interest is the transformation between fcc and bcc, and it has been attributed to the range and steepness of the intermicellar potential.[6]

The pioneering work on the fcc/bcc selection in block copolymer micelles was performed by McConnell *et al.*[6] They employed poly(styrene-*b*-isoprene) (SI) diblock copolymers of various block compositions, f, and degrees of polymerization, N, in the PI-selective solvent decane. The intermicellar potentials were assumed to be parameterized by the ratio of the PI corona layer thickness to the PS core radius, L/R_c. They found that when $L/R_c < 1.5$, the "crew-cut" micelles have a short-ranged intermicellar repulsion, similar to hard spheres, and thus they favor the fcc structure. For "hairy" micelles ($L/R_c > 1.5$), the interactions become softer and long-ranged, which consequently favor the less dense bcc structure.

As a closely related study, Hamley *et al.* performed a systematic study on a series aqueous solutions of poly(ethylene oxide-*b*-butylene oxide) (PEO-PBO) copolymers, denoted PEO_m PBO_n or $PEO_mPBO_nPEO_m$ for diblock or triblock copolymers, respectively, where m and n are degrees of polymerization for PEO and PBO blocks, respectively.[7-9] They used the ratio m/n to represent the relative corona size to the core block. It was shown that the fcc phase is observed at low concentrations for m/n < 10, and the bcc phase for the other case (m/n > 10 and high concentration for m/n < 10). This is qualitatively consistent with McConnell *et al.*[6] Another feature was that all the fcc phases transform to the bcc phase upon increasing concentration, namely, the lyotropic fcc to bcc transition.[7,10] It was ascribed to easier penetration of the

*Corresponding Authors. E-mail: joona@korea.ac.kr or lodge@chem.umn.edu

corona at higher concentrations, based on the argument that the PEO chains at higher concentration will be closer to the theta conditions characteristic of the melt. As a temperature-dependent behavior, they observed the bcc to fcc transition upon heating in $PEO_{40}PBO_{10}$ diblock copolymer in water. It was concluded that the transition is induced by thinning of the corona layer. With increasing temperature, the PEO corona block shrinks, as the water becomes a poor solvent for PEO. Consequently, the intermicellar potential becomes short-ranged, resulting in the fcc phase.

We have mapped out the phase diagrams for several SI diblock copolymers in both PS and PI selective solvents.[11-14] Spherical micelles were observed at dilute regime for all polymers for which f is in the range $0.23 < f < 0.70$, and thus the cubic phases, i.e., fcc or bcc, were formed at higher concentration. In particular the thermotropic fcc to bcc transition was observed in some phase diagrams, and the mechanism and the cause of this transition have been explored recently.[15-18] Based on our observations, Grason proposed a mean-field model to describe the phase behaviors of the cubic lattices in block copolymer micelles.[19] By computing the free energy of micellar phases at various conditions (solvent selectivity and polymer concentration), both the thermotropic and the lyotropic fcc to bcc transitions were predicted. In this case, the thermotropic transition was attributed to the entropic stabilization of the bcc structure near the melting point, whereas the lyotropic transition was considered as a density-driven transition, in which the intermicellar repulsions for the bcc structure is preferred at higher micellar density.

In this paper, we describe the features of the cubic phases in SI block copolymer solutions, such as the fcc/bcc transitions that depend on the block composition, temperature, and concentration, and also compare with the previous experiments and calculations. From the comprehensive data set we have collected, the validity of the McConnell-Gast criterion is discussed in detail. Also, the fcc/bcc transitions in our system are compared with the recent calculation by Grason.

Experimental

Materials. Nine poly(styrene-*b*-isoprene) (SI) diblock copolymers were polymerized by living anionic polymerization using standard procedures.[14] The polymers were characterized by size exclusion chromatography (SEC), using both refractive index (Wyatt Optilab) and multiangle light scattering detectors (Wyatt Dawn), and by ^{1}H-NMR. SEC determined the number average block molecular weights and the polydispersities. ^{1}H-NMR was used to determine the block composition, f, and to estimate the mole percent of 4,1-addition of the PI block (94 ± 1%). The samples were denoted as SI(X-Y), where X and Y represent the PS and PI block molecular weights in kg/mol. Also, "d" in SdI(15-14) and dSI(16-15) indicates that the following block was perdeuterated. The solvents di-*n*-butyl phthalate (DBP), diethyl phthalate (DEP), dimethyl phthalate (DMP), *n*-tetradecane (C14), and squalane (C30) were purchased from Aldrich and purified by vacuum distillation. The polymer solutions were prepared gravimetrically, with the aid of methylene chloride as a cosolvent. The cosolvent was stripped off under a stream of nitrogen at room temperature until a constant weight was achieved. The polymer volume fraction, ϕ, was calculated assuming additivity of volumes and densities of 1.043, 1.118, 1.160, 0.763, 0.810, 1.047, 0.913 g/cm^3 for DBP, DEP, DMP, C14, C30, PS and PI, respectively.

Small Angle X-Ray Scattering (SAXS). SAXS measurements for SI solutions were made on the 2m beam line at the University of Minnesota. CuK_α X-rays ($\lambda = 1.54$ Å) are generated by a Rigaku RU-200BVH rotating anode X-ray generator equipped with an 0.2 × 2 mm microfocus cathode, and collimated with Franks mirror optics. 2D SAXS patterns are detected by a 1024 × 1024 pixel (each pixel = 100 μm^2) Siemens area detector (HI-STAR™ Siemens Analytical X-ray Instruments) at the end of an evacuated flight tube. The sample to detector distance of 2.43 m was used for all measurements. The solutions were sealed within 1.5 or 2.0 mm quartz capillaries using a high temperature silicone based sealant. The measurements were performed by first annealing each sample at a set temperature for at least 600 s, followed by a 300-600 s exposure. The 2-D SAXS images were azimuthally averaged to produce one-dimensional profiles of intensity, I vs. wavevector, q.

Results and Discussion

Previously the phase diagrams of several SI copolymers, SI(11-32), SI(11-21), SI(15-15), SI(15-13), SI(8-7), SI(22-12), and SI(38-14), in both PS and PI selective solvents were constructed as functions of temperature, T, and concentration, ϕ.[12-14] Based on the (T, ϕ) phase diagrams at various f, phase maps on two other planes through the phase cube, such as (ϕ, f) at constant T and (T, f) at constant ϕ, were also determined.[14] Of the numerous features in the resulting phase behaviors, we have focused on the cubic packing of micelles, which is prevalent in the range $0.20 < \phi < 0.40$. Figure 1 displays two (T, f) phase maps for SI copolymers in DEP with $\phi = 0.20$ and 0.30. Cylinders, fcc, fcc/bcc, and bcc are observed with increasing f. For $\phi = 0.20$, the cylinder phase almost disappears and the reentrant order-disorder transitions (ODTs), ordering of micellar solutions onto an fcc or bcc lattice upon heating, are observed. The broad window of cylinder at $\phi = 0.30$ reflects the change of the interfacial curvature due to the solvent swelling of short PS blocks, leading to the lyotropic fcc to cylinder transition with increasing ϕ. For the cubic lattices, the fcc is adopted at small f (crew-cut micelle), SI(11-32) and SI(11-21), and the

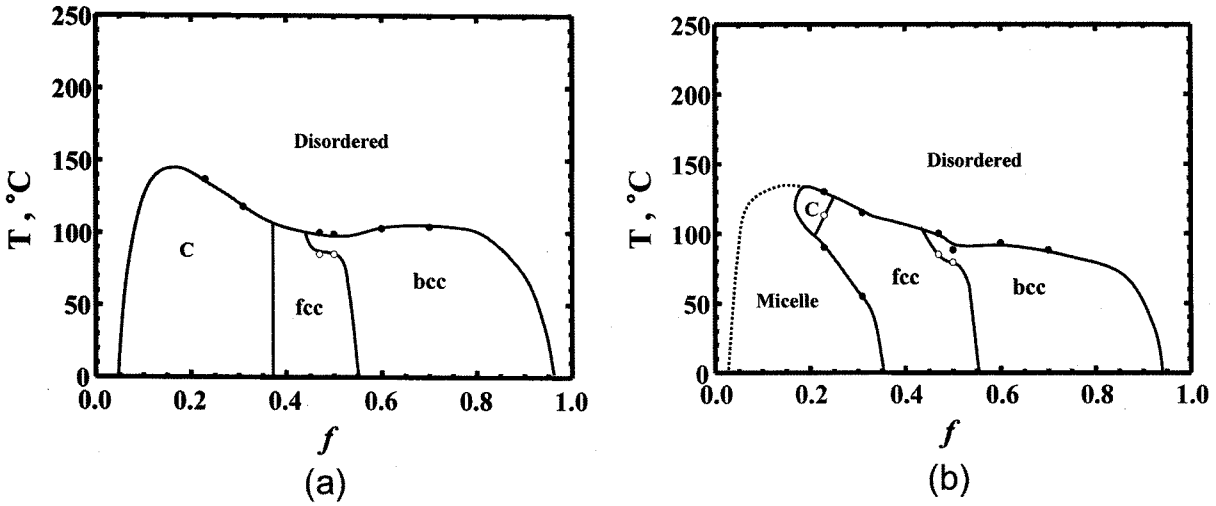

Figure 1. Phase maps for SI diblock copolymers in DEP as functions of temperature, T, and block composition, f, at constant polymer volume fraction, (a) $\phi = 0.30$ and (b) $\phi = 0.20$. Figure updated from reference 11.

bcc is favored at large f (hairy micelle), SI(22-12), and SI(38-14). At intermediate f, i.e., $f \approx 0.5$, the thermotropic fcc to bcc transition upon heating is observed. The fcc/bcc selection at low temperature is qualitatively consistent with the McConnell and Gast conjecture in that the crew-cut micelles, having short-ranged repulsive interactions, prefer fcc, whereas the hairy micelles prefer bcc due to the long-ranged intermicellar potential.[6]

We can also compare the intermicellar potentials more quantitatively by estimating the ratio of the corona layer thickness to the core radius, L/R_c. Table I lists the values of L/R_c measured at ambient temperature for various solutions we previously examined. For protonated SI copolymers, the value of R_c was estimated from the position of the first minimum of the sphere form factor in the SAXS data for $\phi \approx 0.20$ solutions. The SAXS contrast is mainly attributed to the core scattering, and thus the first minimum reflects the core dimension. The overall micellar size was measured from the hydrodynamic radius, R_h, in dilute solution, and L is calculated as $L \approx R_h - R_c$. For SI copolymers with perdeuterated blocks, i.e., SdI(15-14) and dSI(16-15), L/R_c was obtained by fitting the data from small angle neutron scattering (SANS).[18] In the PS selective solvents DEP and DMP, the L/R_c values are in the range between 0.3 and 0.9 for fcc and between 1.1 and 1.4 for bcc, suggesting a transition value of $L/R_c \approx 1.0$ for fcc/bcc selection in this case. This is some-

Table I. Symmetry of Cubic Structures

Copolymer	Solvent	Cubic Lattice	R_h (Å)	R_c (Å)	L/R_c
SI(11-32), $f = 0.23$	DBP	fcc	210	160	0.3
	DEP	fcc	220	160	0.4
SI(11-21), $f = 0.31$	DEP	fcc	191	140	0.4
	C14	bcc	278	89	2.1
SI(15-15), $f = 0.47$	DMP	fcc → bcc	254	136	0.9
	C14	fcc → bcc	205	100	1.1
SI(8-7), $f = 0.49$	DMP	fcc → bcc	150	103	0.5
SdI(15-14), $f = 0.49$	DEP	fcc → bcc	188[a]	103[a]	0.8[a]
	C14	fcc → bcc	218[a]	98[a]	1.2[a]
dSI(16-15), $f = 0.50$	DEP	fcc → bcc	202[a]	114[a]	0.8[a]
	C14	fcc → bcc	230	98	1.3[a]
SI(15-13), $f = 0.50$	DEP	fcc → bcc	150	100	0.5
	DMP	fcc → bcc	150	109	0.4
SI(22-12), $f = 0.60$	DEP	bcc	170	79	1.2
	DMP	bcc	195	91	1.1
SI(38-14), $f = 0.69$	DEP	bcc	197	84	1.4

[a]These values are measured from SANS fit, while the others are from DLS and SAXS.

what less than that of McConnell *et al.*, where $L/R_c = 1.5$ was suggested for SI copolymers in PI selective solvent decane.[6] In the PI selective solvent tetradecane (C14), we found that the micelles pack onto a fcc lattice for the L/R_c value below 1.3, and bcc is formed at $L/R_c = 2.1$, showing a good quantitative agreement with the case of McConnell *et al.* Note that the critical value of $L/R_c = 0.6$ was reported for fcc/bcc transition in chemically modified silver nanoparticles.[20] Therefore, we can conclude that the critical value of L/R_c for fcc/bcc transition varies depending on the system, possibly due to the chemical nature of the corona, whereas the fcc/bcc selection is qualitatively universal in terms of the interparticle potential. Furthermore, Grason suggested recently that the thermodynamics of micellar packing is not sensitive to the core size.[19] From the mean-field model of micellar solutions, he found that intermicellar potentials depend more on the overlap of corona chains that is governed by aggregation number and the effective micellar size, rather than L/R_c, although the McConnell and Gast criterion can broadly explain the fcc/bcc selection.

Apart from the fcc/bcc selection that depends on f, the fcc to bcc transition induced by heating was found in symmetric SI copolymer solutions ($f \approx 0.5$). This transition was observed in both PS and PI selective solvents, and different molecular weight, as represented by phase diagrams, SI(15-15) in DMP and SI(15-15) in C14, in Figure 2. The overall phase behavior reveals the same appearance; the lyotropic phase transition sequence is lamellar (L) → gyroid (G) → cylinder (C) → spheres (S) → micelle, as the solvent is added. The phase boundaries of micelles are different in these phase diagrams, because the effective volume fraction for packing is different, presumably due to the different micellar size. In addition, the lyotropic fcc to bcc transition upon increasing ϕ at low temperature is observed in C14 solution. This was ascribed previously to the relatively longer corona blocks, due to the larger radius of gyration of PI compared to that of PS at equal volume.[18] In this case, it is likely that the micelles become dense at higher ϕ ($\phi > 0.20$) and the corona chains overlap strongly. Hence the bcc is favored, as the entropy penalty for corona overlap is lower in bcc, due to the smaller area of the corresponding Wigner-Seitz cell.[21] The fcc is preferred at lower ϕ ($\phi < 0.20$), where the micelles are less dense and the corona is less likely to overlap. As noted previously, Hamley *et al.* also observed the lyotropic fcc to bcc transition in aqueous solutions of several PEO-PBO copolymers, and we believe that the origin of the transition is same in both systems.[8,9] Recently, this lyotropic behavior was described as an interaction-driven transition.[19] In a mean-field calculation the fcc/bcc phase boundary was observed with increasing ϕ, which was reflected in an unusual behavior of the micellar aggregation number, Q (see Figure 6 in reference 16).[19] At lower ϕ, Q increases linearly with ϕ and the micelles are not dense so that they do not overlap strongly. However, when the system reaches a point

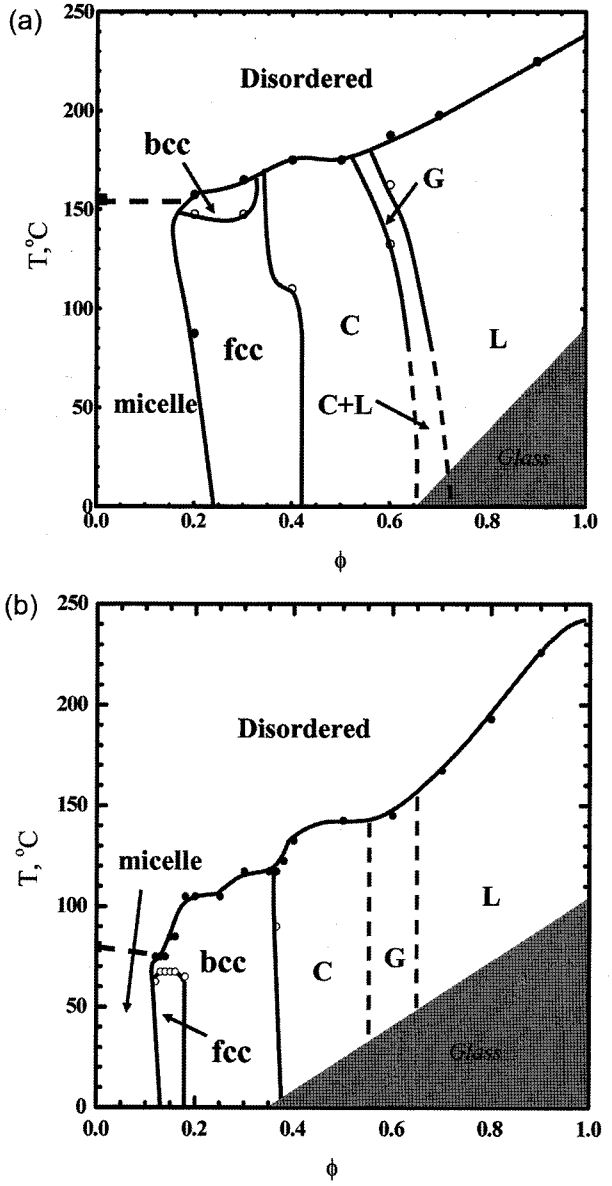

Figure 2. Phase diagrams for (a) SI(15-15) in DMP and (b) SI(15-15) in C14 as functions of temperature, T, and polymer volume fraction, ϕ. Figure 2(a) is reproduced from reference 13, and Figure 2(b) is updated from reference 15.

where strong overlap becomes unavoidable, Q then decreases and the micelle density increases with increasing ϕ. Since the bcc structure is preferred at high densities (also low Q), the lyotropic fcc to bcc transition become feasible (see Figure 2 in reference 16).[19]

For the thermotropic fcc to bcc transition, we have established the mechanism and the cause of this transition previously.[15-18] Figure 3 represents the SAXS profiles showing the thermotropic fcc to bcc transition for solutions in Figure 2, i.e., SI(15-15) in DMP with $\phi = 0.20$ and SI(15-15) in C14 with $\phi = 0.15$. The fcc and bcc phases can be clearly

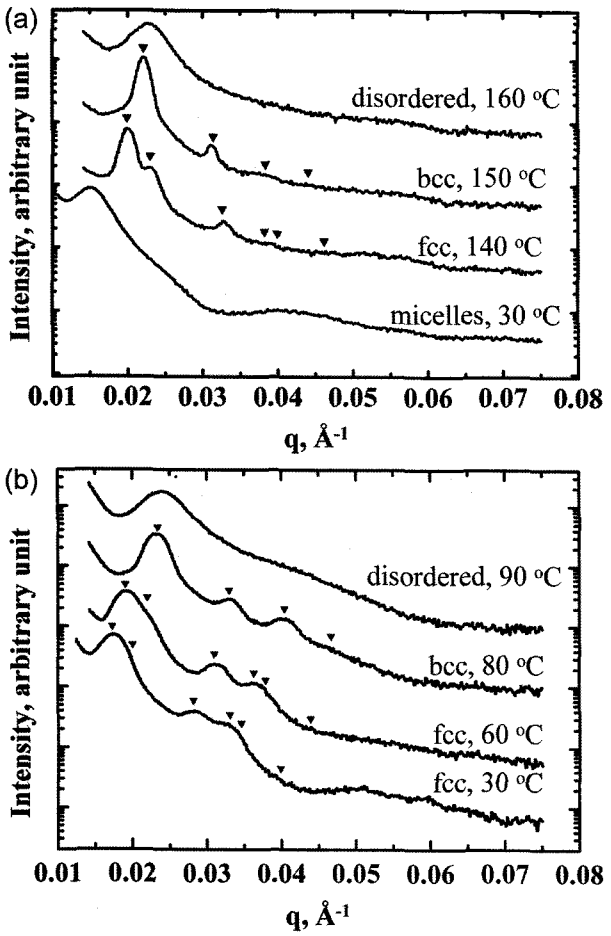

Figure 3. SAXS traces as a function of temperature for SI(15-15) in DMP $\phi = 0.20$ and SI(15-15) in C14 $\phi = 0.15$, which exhibit the thermotropic fcc to bcc transition. The arrows indicate the relative positions for the allowed reflections for fcc and bcc structures.

identified by higher order reflections at $\sqrt{3}$:$\sqrt{4}$:$\sqrt{8}$:$\sqrt{11}$:$\sqrt{12}$:$\sqrt{16}$ and $\sqrt{1}$:$\sqrt{2}$:$\sqrt{3}$:$\sqrt{4}$, respectively. Note that the micellar phase is observed for SI(15-15) in DMP with $\phi = 0.20$ at lower temperature, as evidenced by the absence of higher order peaks. Upon heating, the disordered micelles pack onto fcc phase, then transform to bcc, and disordered (Figure 2(a)). This feature, the reentrant ODT, has been ascribed to the solvent swelling of the micelle core with increasing temperature.[14]

It has been established that the fcc to bcc transition is thermoreversible and epitaxial, and the transformation pathway is identical to that established in atomic systems.[15,16] We also examined the temperature-dependent micellar structures in dilute solutions by employing SANS to see how the values of L/R_c change with increasing temperature, especially across the fcc/bcc boundary.[18] In contrast to the fcc/bcc selection by L/R_c, it was shown that the values of L/R_c essentially remain unchanged over the entire temperature range. This strongly implies that L/R_c is not a factor on the softening of the intermicellar potential upon heating. Instead, this transition is driven by a decrease in the aggregation number, Q, as the solvent selectivity decreases with increasing temperature.[17] By comparing with simulations of highly branched star polymers by Watzlawek *et al.*,[22] it was concluded that a decrease in Q induces a softer intermicellar potential, and thus the fcc to bcc transition occurs. The critical value of Q for the transition in our systems was in the range $70 < Q < 90$, whereas in the simulation on the star polymers it was predicted to be $60 < Q < 70$. Our result is consistent with recent theoretical calculation by Grason, in that the thermotropic fcc to bcc transition can be described by same origin.[19] The dissolution of micelles with increasing temperature leads to the decrease in Q (to reduce the micellar repulsion) and thereby the increase in the micelle density (see reference 14 for the detailed values).[17] As a consequence, both effects enhance the stability of the bcc structure near the ODT.

The last aspect to consider is the general characteristics of this transition from the data collected. Figure 4 represents a plot of the normalized nearest neighbor distance, R_{nn}/R_{nn}^*, as a function of a normalized distance of the styrene-isoprene-interaction parameter from the ODT, $(\chi - \chi_{ODT})/\chi_{ODT}$, for SI(15-15) in various solvents exhibiting the fcc to bcc transition, where R_{nn}^* is R_{nn} in the regime of constant micellar dimension (usually at ambient temperature), and $\chi = 33/T - 0.0228$ was used for the expression of χ.[23] From this master plot, it can be seen that the fcc to bcc transition occurs in the range $0.85 < R_{nn}/R_{nn}^* < 0.93$, and $0.004 < \chi - \chi_{ODT} < 0.007$. Also, there are three distinct regimes in the plot; the fcc lattice with nearly constant R_{nn} at low temperature, the fcc with decreasing R_{nn}, and the bcc lattice with decreasing R_{nn}. The temperature region of the constant R_{nn} is consistently observed in the dilute solutions, and we proposed that, in this regime, the

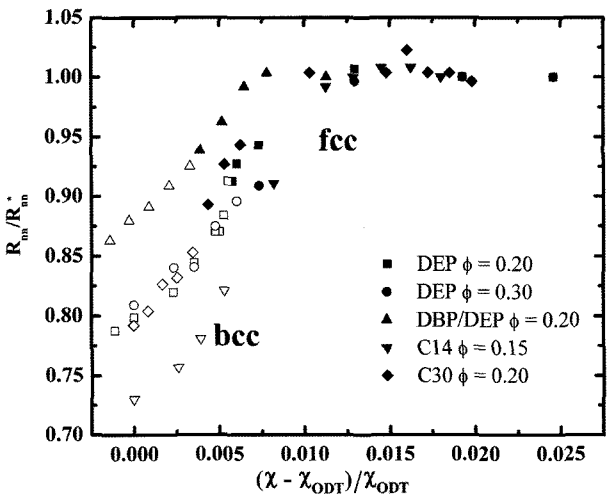

Figure 4. A plot of R_{nn}/R_{nn}^* vs $(\chi - \chi_{ODT})/\chi_{ODT}$ for solutions exhibiting the thermotropic fcc to bcc transition. The filled and open symbols indicate fcc and bcc phases, respectively.

aggregation number remains constant due to the entropy penalty of the core chains.[18] This regime becomes more apparent when the micelles persist up to higher temperature, and, in this case, a slight increase in R_m due to the solvent swelling is often observed, which often induces the reentrant ODT. Once the micellar size begin to decrease, then the fcc to bcc transition occurs before the micelles melt away. Following the each data set, it can be viewed that the fcc/bcc boundary lies halfway between the onset of decreasing R_m and the ODT.

Conclusions

In this paper, the fcc/bcc selection among various SI diblock copolymer micelles has been described. Qualitatively, it follows the McConnell and Gast scenario,[6] as crew-cut micelles favor a fcc lattice and hairy micelles prefer a bcc lattice. However, it was pointed out that the criterion of "$L/R_c = 1.5$" is not a determining factor. Instead, the recent mean-field calculation suggested that the intermicellar potential depends more on the solvation properties of the copolymers (i.e., aggregation number and micellar size) than L/R_c *per se*. As an intriguing feature, the lyotropic and the thermotropic fcc to bcc transition has been also considered. The lyotropic transition was observed as the polymer concentration increases, and it was described as the interaction-driven transition at higher micellar density. The thermotropic transition was found in nearly symmetric SI copolymers in both PS and PI selective solvents. The mechanism and the cause of this transition have been investigated extensively. This transition is induced by a decrease in the solvent selectivity with increasing temperature. As a consequence, the aggregation number decreases and the micelle density increases, leading to a stabilization of the bcc structure near the ODT, as evidenced by both experiments and calculations.

Acknowledgements. This work was supported by a Korea University Grant (K0616581), and by the MRSEC Program of the National Science Foundation under Award Number DMR-0212302.

References

(1) I. W. Hamley, *The Physics of Block Copolymers*, Oxford University Press, New York, 1998.
(2) P. Alexandridis and B. Lindman, *Amphiphilic Block Copolymers: Self-Assembly and Applications*, Elsevier Science B.V., Amsterdam, 2000.
(3) C. S. Cho, I. K. Park, J. W. Nah, and T. Akaike, *Macromol. Res.*, **11**, 2 (2003).
(4) S. W. Hong, K. H. Kim, J. Huh, C. H. Ahn, and W. H. Jo, *Macromol. Res.*, **13**, 397 (2005).
(5) W. S. Shim, J. S. Lee, and D. S. Lee, *Macromol. Res.*, **13**, 344 (2005).
(6) G. A. McConnell, A. P. Gast, J. S. Huang, and S. D. Smith, *Phys. Rev. Lett.*, **71**, 2102 (1993).
(7) J. A. Pople, I. W. Hamley, J. P. A. Fairclough, A. J. Ryan, B. U. Komanschek, A. J. Gleeson, G. E. Yu, and C. Booth, *Macromolecules*, **30**, 5721 (1997).
(8) I. W. Hamley, C. Daniel, W. Mingvanish, S.-M. Mai, C. Booth, L. Messe, and A. J. Ryan, *Langmuir*, **16**, 2508 (2000).
(9) I. W. Hamley, S.-M. Mai, A. J. Ryan, J. P. A. Fairclough, and C. Booth, *Phys. Chem. Chem. Phys.*, **3**, 2972 (2001).
(10) I. W. Hamley, J. A. Pople, and O. Diat, *Colloid Polym. Sci.*, **276**, 446 (1998).
(11) I. W. Hamley, J. P. A. Fairclough, A. J. Ryan, C. Y. Ryu, T. P. Lodge, A. J. Gleeson, and J. S. Pedersen, *Macromolecules*, **31**, 1188 (1998).
(12) K. J. Hanley and T. P. Lodge, *J. Polym. Sci.; Polym. Phys. Ed.*, **36**, 3101 (1998).
(13) K. J. Hanley, T. P. Lodge, and C.-I. Huang, *Macromolecules*, **33**, 5918 (2000).
(14) T. P. Lodge, B. Pudil, and K. J. Hanley, *Macromolecules*, **33**, 5918 (2002).
(15) J. Bang, T. P. Lodge, X. Wang, K. L. Brinker, and W. R. Burghardt, *Phys. Rev. Lett.*, **89**, 215505/1 (2002).
(16) J. Bang and T. P. Lodge, *J. Phys. Chem. B*, **107**, 12071 (2003).
(17) T. P. Lodge, J. Bang, M. J. Park, and K. Char, *Phys. Rev. Lett.*, **92**, 145501 (2004).
(18) J. Bang, K. Viswanathan, T. P. Lodge, M. J. Park, and K. Char, *J. Chem. Phys.*, **121**, 11489 (2004).
(19) G. M. Grason, *J. Chem. Phys.*, **126**, 114904/1 (2007).
(20) B. A. Korgel and D. Fitzmaurice, *Phys. Rev. B*, **59**, 14191 (1999).
(21) P. Ziherl and R. D. Kamien, *J. Chem. Phys. B*, **105**, 10147 (2001).
(22) M. Watzlawek, C. N. Likos, and H. Löwen, *Phys. Rev. Lett.*, **82**, 5289 (1999).
(23) T. P. Lodge, C. Pan, X. Jin, Z. Liu, J. Zhao, W. W. Maurer, and F. S. Bates, *J. Polym. Sci.; Polym. Phys. Ed.*, **33**, 2289 (1995).